



## Ultrasonic processing of enzymes: Effect on enzymatic activity of glucose oxidase

Anthony Guiseppi-Elie<sup>a,b,c,\*</sup>, Sung-Ho Choi<sup>a,d</sup>, Kurt E. Geckeler<sup>a,d</sup>

<sup>a</sup> Center for Bioelectronics, Biosensors and Biochips (C3B), Clemson University, 100 Technology Drive, Anderson, SC 29625, USA

<sup>b</sup> Department of Chemical and Biomolecular Engineering, Clemson University, Clemson, SC 29634, USA

<sup>c</sup> Department of Bioengineering, Clemson University, Clemson, SC 29634, USA

<sup>d</sup> Department of Materials Science and Engineering, Gwangju Institute of Science and Technology (GIST), Gwangju 500-712, South Korea

### ARTICLE INFO

#### Article history:

Received 30 July 2008

Received in revised form 8 December 2008

Accepted 8 December 2008

Available online 24 December 2008

#### Keywords:

Ultrasonication

Enzyme activity

Glucose oxidase

Enzyme processing

### ABSTRACT

The effect of ultrasonication on the enzymatic stability, conformation, and catalytic activity of the important oxidoreductase, glucose oxidase (GOx), was investigated. Thus, buffer-free aqueous solutions of GOx were ultrasonicated (23 kHz at 4 °C) for different periods of time (10, 30, and 60 min) and studied in terms of their enzymatic activity. The ultrasonicated GOx was also studied by UV/vis and circular dichroism (CD) spectroscopy and by thermogravimetric analysis, and compared with pristine GOx. The CD spectra of ultrasonicated GOx showed a different composition with reduced  $\alpha$ -helix and  $\beta$ -sheet fractions upon extended sonication compared with the pristine GOx. Along with the changes of the secondary structure, the enzymatic activity measured via HRP-coupled bioassay of the sonicated GOx showed a small corresponding decrease. Low temperature ultrasonic processing of GOx does not appreciably compromise bioactivity.

© 2009 Elsevier B.V. All rights reserved.

### 1. Introduction

Recent developments in the processing and biofunctionalization of nanomaterials such as carbon nanotubes, fullerenes, dendrimers, and cyclodextrins, have attracted much attention across scientific and engineering disciplines because of their fascinating potential for altering conventional bulk materials in micro and nanoelectronic devices, in chemical and biological sensors and in targeted drug delivery. In order to synthesize and process functional bionanomaterials [1] two general approaches can be utilized: one is the covalent approach and the other is the non-covalent approach, including supramolecular strategies, which are regulated by supramolecular interactions such as hydrogen bonding,  $\pi$ - $\pi$  stacking, hydrophobic effects, etc. [2]. The latter approach is considered particularly interesting, because it can potentially preserve the physico-chemical properties of the pristine nanomaterials and biomaterials following supramolecular assembly compared with covalent conjugation pursuant to chemical modification of intact nanomaterials [3].

One of the most popular and prioritized pathways for non-covalent approaches to achieve biological functionalization of

nanomaterials is by liquid-phase reactions based on ultrasonication [4]. Ultrasonication is the use of high-intensity acoustic energy to process materials and has become a favored route to the processing of biologically functionalized nanomaterials. Despite the widespread use of ultrasonication in various research disciplines as well as industry, surprisingly, the effects of ultrasonic energy on the stability and function of proteins, particularly enzymes, were reported only rarely [5,6]. Indeed, even though many factors such as temperature [7], pH [8], buffer systems [9], solvents [10], purity [11], and isoelectric point [12], can affect the stability and function of biomacromolecules, the effects of ultrasonication on biomolecules can have similar, important, and far-reaching implications. Such implications go to the use of ultrasonic power in nanobiotechnology related research fields, especially when it is a prerequisite tool in the processing of biofunctionalized nanomaterials. The present work deals with the investigation of the effects of ultrasonic power on solutions of the commercially important enzyme, glucose oxidase. Glucose oxidase was selected because its association with single-walled carbon nanotubes has been shown to mediate or result in direct electron transfer between the flavin cofactor of the enzyme and SWNT-based electrodes [13].

Ultrasonicated and pristine GOx were studied by UV/vis spectroscopy, thermogravimetric analysis, circular dichroism, and colorimetric enzymatic bioactivity assay. Our motivation is to understand what effect, if any, this processing method has on the bioactivity of the enzyme. GOx is a relatively broadly utilized enzyme [14] because of its spectrum of applications in biosensors

\* Corresponding author at: Center for Bioelectronics, Biosensors and Biochips (C3B), Clemson University, 100 Technology Drive, Anderson, SC 29625, USA. Tel.: +1 864 656 1712; fax: +1 864 656 1713.

E-mail address: [guiseppi@clemson.edu](mailto:guiseppi@clemson.edu) (A. Guiseppi-Elie).

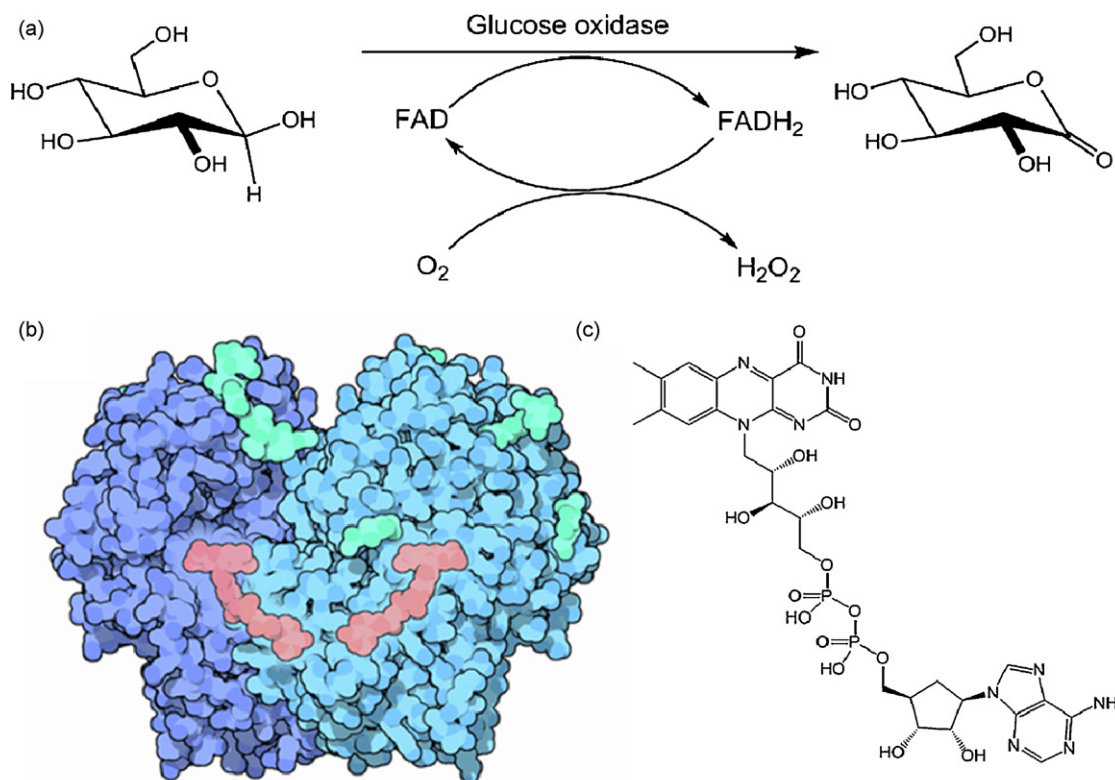


**Fig. 1.** (a) Scheme of the enzymatic reaction based on GOx, (b) molecular model of GOx (GOx with two subunits depicted as dark- and light-blue, while the FAD coenzyme is depicted in pink), and (c) the molecular structure of FAD [22]. (For interpretation of the references to color in this figure legend, the reader is referred to the web version of the article.)

for medical applications [15], environmental monitoring [16] as well as for its potential in the next generation biofuel cell systems [17]. In addition, there are applications in the food industry, such as an additive for food processing [18], antioxidant [19], preservative as oxygen scavenger [20], and use in wine [21].

GOx (β-D-glucose oxygen-1-oxidoreductase, EC 1.1.3.4) from *Aspergillus niger* is a flavoenzyme that catalyzes the oxidation of β-D-glucose to δ-gluconolactone through a two-step reaction (Fig. 1(a)). In the beginning of the reaction, β-D-glucose is oxidized to δ-gluconolactone by the glucose oxidase cofactor, flavin adenine dinucleotide (FAD) (Fig. 1(b)) which in turn is reduced to FADH<sub>2</sub>. In the second step, oxygen is reduced to hydrogen peroxide, and FADH<sub>2</sub> is reoxidized to FAD. Structurally, the enzyme is a homodimer of two identical subunits with a molecular weight of 160 kg/mol. The dimer contains one tightly, non-covalently bound FAD cofactor, one free sulfhydryl group, and one disulfide bond per monomer. Under deactivating conditions, the subunits of GOx dissociate accompanied by the loss of the FAD cofactor (Fig. 1(c)) [22].

## 2. Experimental

### 2.1. Materials and reagents

GOx (EC 1.1.3.4) from *A. niger* (type VII-S, 150,000 units/g solid) was purchased from Sigma and used as received. According to Sigma, the lyophilized powder contained approximately 80% protein. To measure the GOx enzymatic activity by the glucose oxidase-horseradish peroxidase (HRP) coupled enzyme reaction bioassay system [23], HRP (EC 1.11.1.7, Type II, 220 purpurogallin units/mg solid) was purchased from Sigma. The 96-well microtitre plates for enzymatic assays were purchased from Falcon. Sodium acetate trihydrate, *o*-dianisidine dihydrochloride, were from Sigma;

β-D-(+)-glucose anhydrous was from Fluka. The D.I. water was produced using a Milli-Q® Ultrapure Water Purification System.

### 2.2. Apparatus

Ultratip sonication of the aqueous enzyme solution was performed using a Soniprep 150 (MSE, UK) equipped with a standard probe (diameter: 9.5 mm, transformation ratio 5.5:1). The UV/vis spectra of aqueous enzyme solutions were obtained with a Cary 300 spectrophotometer (Varian, Inc.). The lyophilization of the aqueous enzyme solutions was carried out with a VirTis Benchtop 6K freeze dryer (VirTis, Inc.). Thermogravimetric analysis (TGA) data were recorded on a TGA 7 instrument (PerkinElmer, Inc.). An ELISA plate reader (Powerwave XS, Bio-Tek, Inc.) was used in the kinetics mode for the enzyme activity assays. Circular dichroism (CD) measurements were made with a Jasco J-810 automatic recoding spectropolarimeter fitted with a xenon lamp.

### 2.3. Methods

#### 2.3.1. UltraTip sonication

Aqueous GOx solutions were prepared in 15 mL D.I. water (concentration: 1 mg/mL), then sonication was performed with the ultratip sonicator (frequency: 23 kHz). Triplicate solutions were sonicated continuously for 10, 30, or 60 min, respectively, in an ice-cooled water bath. After the tip sonication each sample was immediately transferred to and kept in the refrigerator at 4 °C.

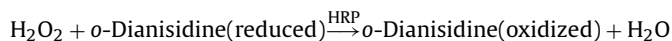
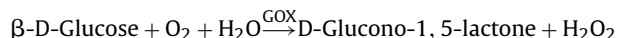
#### 2.3.2. UV/vis spectroscopy and thermogravimetric analysis

An aliquot of 3 mL of the sonicated aqueous GOx solution (sGOx) was transferred to a quartz cuvette and the UV spectra were recorded for a wavelength range of 240–550 nm. An aqueous GOx solution served for the control experiment. In order to prevent light

scattering from small particles, the solutions were maintained dust-free and degassing was performed before the measurements. As many buffers and common buffer additives absorb in the far-UV region, buffer-free aqueous GOx solutions were used, so that the concentrations of GOx could be calculated without further correction. The TGA curves of solid samples ( $n=3$ ) were obtained in a  $N_2$  atmosphere at a heating rate of  $10^\circ\text{C min}^{-1}$  from 20 to  $770^\circ\text{C}$ .

### 2.3.3. Enzymatic assay

Both the sGOxs and (pristine) GOx samples were subjected to triplicate bioassays at  $35^\circ\text{C}$  using the HRP-coupled assay [23], in which the reaction catalyzed by the subject enzyme is linked to the decomposition of hydrogen peroxide with HRP and the oxidation of the chromogenic reagent, *o*-dianisidine:



The following reagents were used for the conduct of the enzyme assay: (A) 50 mM sodium acetate buffer at  $35^\circ\text{C}$ , pH 5.1 adjusted with 1 M HCl; (B) 0.21 mM *o*-dianisidine in reagent A; (C) various concentrations of  $\beta\text{-D-glucose}$  from 10 to  $1000\ \mu\text{M}$  in D.I. water; (D) mixed reaction cocktails of reagent B and C and equilibrated to  $35^\circ\text{C}$  and adjusted to pH 5.1 with 1 M HCl or 1 M NaOH; (E) HRP solution containing 60 purpurogallin units/mL in cold D.I. water; (F) double-step diluted pristine and sGOx solutions ( $4\ \mu\text{g/mL}$ ) in reagent A. The reactions were carried out by mixing 0.29 mL of freshly prepared D and 0.01 mL of E, maintaining the mixture for 10 min at  $35^\circ\text{C}$  to equilibrate the absorbance at 500 nm, and then adding 0.01 mL of F followed by recoding the increase of the absorbance at 500 nm every 15 s over a period of 15 min maximum. One enzyme unit is defined as the amount of enzyme required to oxidize  $1\ \mu\text{mol}$  of  $\beta\text{-D-glucose}$  per min at  $35^\circ\text{C}$ . The initial rate data obtained were used to determine the kinetic parameters ( $V_{\text{max}}$ ,  $K_m$ ,  $n$ ,  $k_{\text{cat}}$ , and  $k_{\text{cat}}/K_m$ ) through non-linear curve fitting of the Hill function algorithm, and the Lineweaver–Burk plot in connection with the Michaelis–Menten equation, using Prism 3.5 software with default settings (GraphPad Software, Inc.). Statistical analysis of replicate data via *t*-test statistic was used to establish a *p*-value.

### 2.3.4. Circular dichroism

The CD measurements were conducted at  $25^\circ\text{C}$  and the scans are the average of three runs at a scan rate of  $10\ \text{nm/min}$ . The secondary structures of pristine and sGOx of different ultrasonication times were analyzed using the computer program, SELCON3 [24], which calculates the structural component ratio of secondary structures for the protein. The mean residue ellipticity  $[\theta]_{\text{MRW}}$  was calculated using a value of 115 for the mean residue mass of GOx.

## 3. Results and discussion

Ultrasonication at 23 kHz causes a temperature increase up to ca.  $35^\circ\text{C}$  within 5 min and further prolonged sonication can increase the temperature of aqueous solutions up to more than  $60^\circ\text{C}$  [25]. Thermally induced denaturation of GOx occurs at  $55.8 \pm 1.2^\circ\text{C}$ , resulting in the physical dissociation of the flavin cofactor from the apoenzyme [26]. In order to eliminate the possible confounding effects of thermal denaturation, all samples were ultrasonicated at ice bath temperatures.

In order to determine the effect of ultrasonication on sGOx, including its possible partial aggregation, partial denaturation, or ultrasonically induced self-chemical modification involving reactions of its UV-absorbing amino acidic residues, UV/vis absorption spectrophotometry analyses were performed. The UV/vis spectra

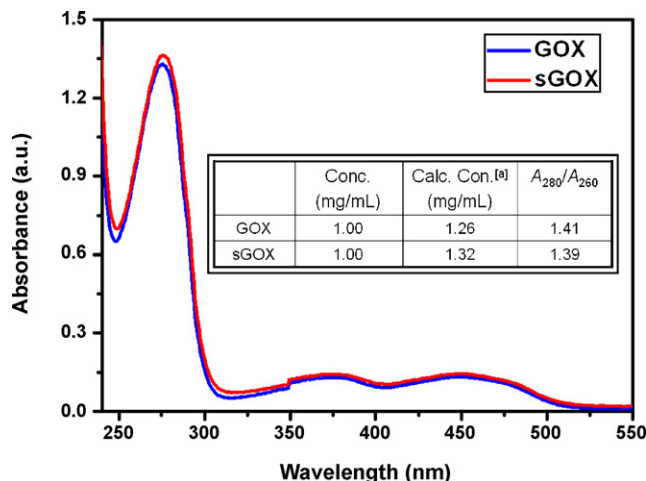


Fig. 2. UV/vis spectra of GOx and sGOx (inset table shows the comparison with the calculated concentrations of GOx and sGOx by using the spectrophotometric method and  $A_{280}/A_{260}$  ratios) [a]:  $C_{\text{protein}} = 1.55 A_{280\text{ nm}} - 0.76 A_{260\text{ nm}}$ .

over the range from 230 to 550 nm of aqueous solutions of pristine and sGOx ( $1\ \text{mg/mL}$ ) after 30 min of ultrasonication are shown in Fig. 2. The absorbance of solutions in the spectral region of 320 and 400 nm remained less than 0.05 a.u., which means both GOx samples were essentially the same and maintained their global protein structure without appreciable chemical modification. Also, the principal absorption peak of both GOx samples was retained at around 280 nm. The values of the  $A_{280}/A_{260}$  ratio were near to 1.5, which means no other chemical contamination [27] or modification occurred. This result shows that ultrasonically treated GOx keeps the overall global chemical composition and structure.

Fig. 3 shows the TGA curves of GOx and sGOx that had been likewise ultrasonicated for 30 min. The TGA curves of both types of samples show two very well differentiated steps. The first transition (GOx and sGOx 2.5 and 3.0% mass loss, respectively) occurred between 25 and  $100^\circ\text{C}$ , and is associated with the broad endothermic effect of the protein. The slight difference between GOx and sGOx may be caused by the combined ultrasonication and local lyophilization of sGOx for the TGA sample preparation compared to the procedures used for commercially acquired GOx. However, technical replicates ( $n=3$ ) established  $p=0.10$  between data sets suggesting a 90% confidence level that these are different samples. The plateau phases of both TGA curves over  $100\text{--}200^\circ\text{C}$  can be rec-

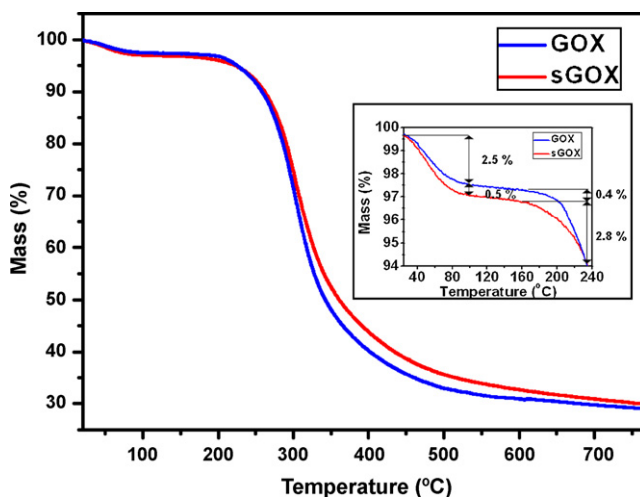
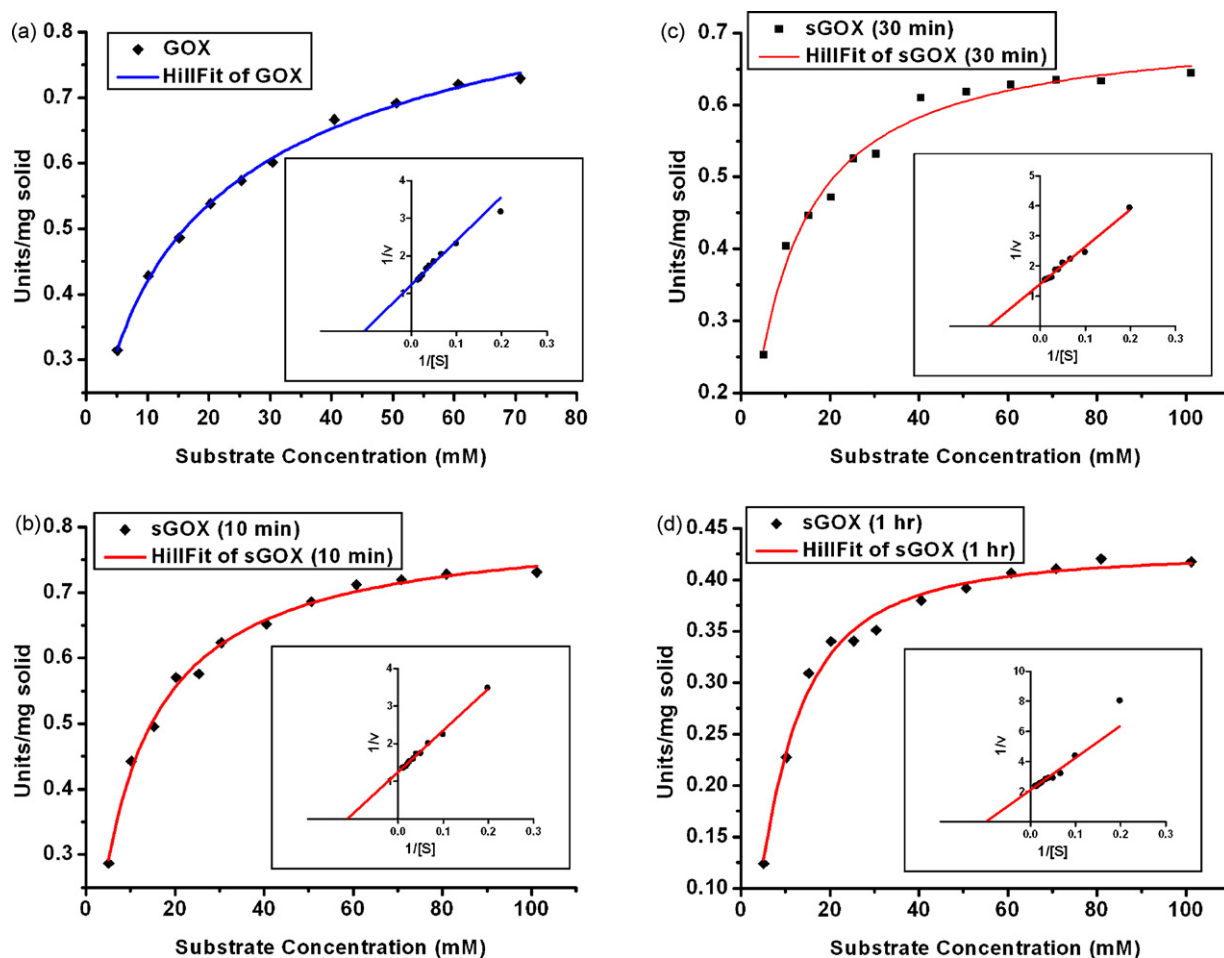


Fig. 3. TGA curves of GOx and sGOx (inset is the magnified region of the curve for the temperature range of  $25\text{--}245^\circ\text{C}$ ).



**Fig. 4.** The Hill fitting results of the enzyme assays of (a) GOx, (b) sGOx – 10 min, (c) sGOx – 30 min, and (d) sGOx – 60 min (each inset from Fig. 5(a–d) shows the Lineweaver–Burk plots of GOx and sGOxs).

ognized as the familiar dehydration process of protein samples, followed by the melting and decomposition process of the protein at more than 200 °C. In the inset of Fig. 4, the small difference of both TGA plateaus is evidence for a slight difference in the amount of water associated with the enzyme that may arise from a slight conformational change of protein provoked by the alteration of secondary structure before and after sonication. It is worth mentioning that two different types of water are present in proteins [28]: (i) the hydration water that is strongly hydrogen-bonded to the protein and (ii) a more weakly bonded water, which is removed at a lower temperature than the former. It is plausible to assume that the latter water molecules would be more abundantly bonded to the altered surface of the enzyme if its overall topology is altered in un-buffered water by ultrasonic energy. The second step, with a major mass loss of ca. 43% is assigned to the thermal decomposition of the protein. The overall shapes of both TGA curves show a similarity and the residues of GOx and sGOx were 29.9 and 29.1%, respectively, which means that the identity of both samples are essentially the same and that sGOx showed only small changes of its conformational structure compared with GOx.

In order to investigate the effect of the slight conformational change of the enzyme by ultrasonication power implied from the result of the TGA, we conducted enzyme activity assays of GOx and sGOx prepared at different sonication times of 10, 30 and 60 min. Because the enzyme function and the fidelity of the active site are strongly connected to the overall structure of the enzyme, this experiment is important to confirm the retained biological function before and after ultrasonication. With this objective, the enzyme

activity assays of all sGOx samples were carried out using the GOx–HRP coupled enzyme reaction system. Fig. 4(a–d) show the results of the enzyme assays of pristine and sGOx.

The enzyme kinetic parameters were determined using varying concentrations of  $\beta$ -D-glucose at constant GOx and sGOx concentrations and by using both the Lineweaver–Burk and Hill plot methods for comparative purposes. A similar Michaelis–Menten curve was obtained when the initial reaction rate of  $\beta$ -D-glucose consumption was plotted against the  $\beta$ -D-glucose concentration. From these data, the kinetic parameters ( $V_{\max}$ ,  $K_m$ ,  $k_{\text{cat}}$ , and  $k_{\text{cat}}/K_m$ ) were determined using the Lineweaver–Burk plot. It is worth mentioning that both  $V_{\max}$  and  $K_m$  will vary at least 10-fold and by calculating the turnover number of the enzyme ( $k_{\text{cat}}$ ) from the  $V_{\max}$  and the enzyme concentration ( $C_{E,\text{total}}$ ) [ $k_{\text{cat}} = V_{\max}/C_{E,\text{total}}$ ], a comparison of the specificity constants ( $k_{\text{cat}}/K_m$ ) (a reflection of the efficiency of the enzyme) and  $K_m$  could be investigated for the validity of the enzyme activity assay. The  $K_m$  and  $k_{\text{cat}}/K_m$  of pristine and sGOx (with sonication times of 10, 30, and 60 min) are presented and compared to literature values in Table 1. Literature values for  $K_m$  and  $k_{\text{cat}}/K_m$  of GOx cover the range 10–18 mM and 20–40 ( $\text{s}^{-1} \text{mM}^{-1}$ ), respectively [29,30]. The  $K_m$  and  $k_{\text{cat}}/K_m$  of GOx and sGOx obtained in this work using the Hill and Lineweaver–Burk plot methods are generally consistent with literature values. However, both the  $V_{\max}$  and  $k_{\text{cat}}$  values of sGOx decreased upon ultrasonication, showing a steady decrease with increasing sonication times of 10, 30, and 60 min.  $V_{\max}$  is significantly altered ( $p < 0.05$ ) following 60 min of ultrasonication. The  $K_m$  values on the other hand show a stepwise decrease, being approximately the



**Table 1**Kinetic parameters of GOx and sGOx using the enzyme-linked assay by the Hill plot and Lineweaver–Burk plot ( $n = 3$  or  $5$ ) and comparison to literature values.

Method	$V_{\max}$ (U mg solid <sup>-1</sup> )	$K_m$ (mM)	$n$	$k_{\text{cat}}$ (s <sup>-1</sup> ) <sup>a</sup>	$k_{\text{cat}}/K_m$ (s <sup>-1</sup> mM <sup>-1</sup> ) <sup>b</sup>
GOx					
Hill	1.03 ± 0.064	17.65 ± 3.53	0.66 ± 0.05	429.17	24.32
L–Burk	0.82 ± 0.017	9.57 ± 0.75	1	341.67	35.70
10 min sGOx					
Hill	0.81 ± 0.061	8.98 ± 0.51	0.99 ± 0.07	337.50	37.58
L–Burk	0.80 ± 0.008	8.93 ± 0.38	1	333.33	37.32
30 min sGOx					
Hill	0.71 ± 0.029	8.83 ± 0.84	0.99 ± 0.12	295.83	33.50
L–Burk	0.71 ± 0.011	8.82 ± 0.61	1	295.83	33.54
60 min sGOx					
Hill	0.43 ± 0.009	9.02 ± 0.44	1.48 ± 0.12	179.17	19.86
L–Burk	0.47 ± 0.012	10.12 ± 1.06	1	195.83	19.35
Lit. [29,30]					
M–Menten	5–240.5	10–18.4	1	741	20–40.27

<sup>a</sup>  $k_{\text{cat}}$  is the enzyme catalytic constant (turnover number);  $k_{\text{cat}} = V_{\max}/C_{E,\text{total}}$  ( $C_{E,\text{total}}$  was calculated as the 60% efficiency compared with the O<sub>2</sub>-saturated reaction).<sup>b</sup>  $k_{\text{cat}}/K_m$  is enzyme specificity constant or enzyme efficiency.

same regardless of sonication time but showing a 50% decrease compared to pristine GOx. Both the  $K_m$  and  $k_{\text{cat}}$  values are significantly altered ( $p < 0.05$ ) following ultrasonication. It should be pointed out that the Michaelis–Menten equation makes certain assumptions regarding the kinetic model of enzyme catalysis, the Hill model does not. The parameter  $n$  of the Hill model approaches the MM model as  $n \rightarrow 1$ . The Hill parameter for pristine GOx was found to be 0.66 suggesting that GOx does not conform to MM kinetics; although it is widely investigated in the literature using this model. Upon ultrasonication, the Hill parameter was found to be 0.99 (10 min), 0.99 (30 min) and 1.48 (60 min) suggesting that upon short duration ultrasonication, the physicochemical changes of the enzyme makes its kinetics better conform to the MM model. These results clearly show that upon ultrasonication, the enzyme activity of GOx is mostly preserved; however, subtle changes in its structure following an extended ultrasonication time may reduce the activity significantly.

Finally, in order to understand the conformational changes of sGOx and its relation to the retention of the enzyme activity after different sonication intervals, circular dichroism spectra were studied. The results of the analysis of the CD spectra of pristine and sGOx are shown in Fig. 5 and are summarized in Table 2, which gives the relative amounts for each structural component of the pristine GOx and sGOx.

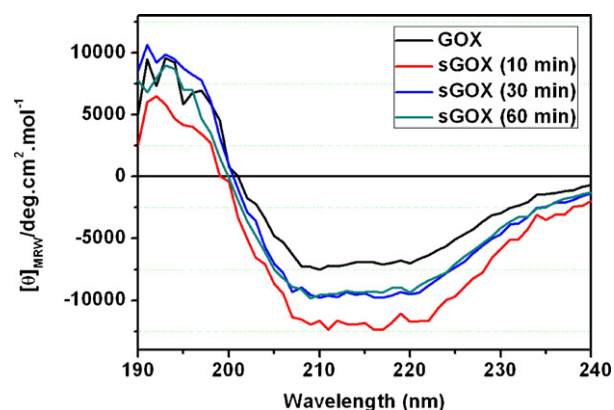
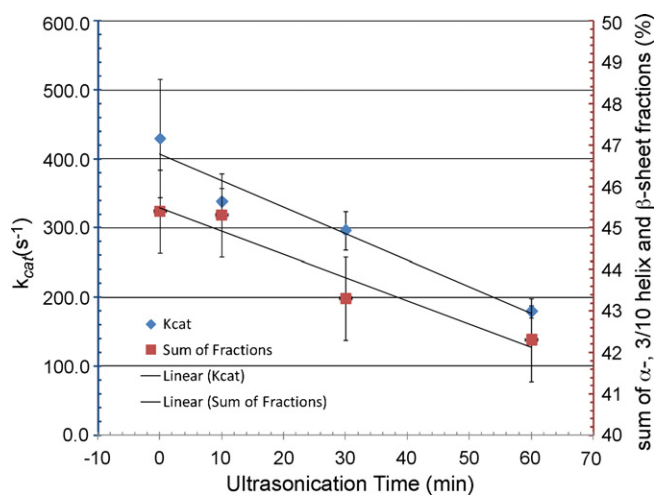
This analysis shows that the sum of the fraction of  $\alpha$ -helices and the fraction of  $\beta$ -sheets was reduced with an increase of the sonication time (see the value of  $(\alpha \text{ Hel} + 3/10 \text{ Hel}) + \beta$ ). Such a decrease of the sum of  $\alpha$ -helical and  $\beta$ -sheet fractions in GOx as a result of the ultrasonic treatment can be seen as a release of surface pressure [31] and the induced structural transformations, which may affect the active site of the enzyme.

In order to investigate the relationship between the secondary structure and the enzyme activity as a function of the sonication time, another plot was created. Fig. 6(a) shows the  $k_{\text{cat}}$  value and the sum of the  $\alpha$ -, 3/10 helix and  $\beta$ -sheet fractions for different sonication times. Both the  $k_{\text{cat}}$  and the sum of fractions are observed to decrease monotonically with ultrasonication times.

**Table 2**

Secondary structure of GOx and sGOxs in D.I. water.

SELCON3	$\alpha$ -helix	3/10 helix	$\beta$	$\alpha + \beta$	Turn	Poly(Pro)II	Random-coil
GOx	13.0	6.2	26.2	45.4	14.2	5.9	33.6
10 min sGOx	19.9	5.7	19.7	45.3	13.3	6.3	35.7
30 min sGOx	22.2	5.0	16.1	43.3	13.2	7.0	37.0
60 min sGOx	18.7	5.5	18.1	42.3	13.5	6.8	36.7

**Fig. 5.** Far-UV CD spectra of GOx and sGOx.**Fig. 6.** (a)  $k_{\text{cat}}$  value and the sum of  $\alpha$ -, 3/10 helix and  $\beta$ -sheet fractions vs. sonication time.

#### 4. Conclusions

The process of ultrasonication at 23 kHz for periods up to 1 h does not appear to adversely affect the enzymatic activity of the oxidoreductase enzyme, GOx. The present study was based on buffer-free, aqueous solutions, which is the simplest biological fluidic system possible. These GOx enzyme aqueous solutions treated with different ultrasonication times and the conformational structures, secondary structure fractions and enzyme activities were characterized by TGA, UV/vis, CD spectroscopy, and enzyme-linked bioactivity assay. The enzyme appears to maintain its essentially globular topology with subtle changes in its secondary structure that monotonically reduces  $k_{\text{cat}}$  and that was associated with a slight increase in the random coil conformations and a slight decrease in the secondary fractions upon extended ultrasonication. This system may be further improved with due consideration of the forces involved in the sonified fluid and of the use of optimized buffers, pH, temperature, and ionic strength that may prove useful for the processing and design of non-covalent functional supramolecular nanomaterials. This is particularly relevant when consideration is for the non-destructive processing of supramolecular nanomaterials such as oxidoreductase-SWNT conjugates that must preserve the functionality of the biomolecules. These results might also be extended to other biologically relevant members of the oxidoreductase family such as lactate oxidoreductase and alcohol oxidoreductase.

#### Acknowledgements

This work was supported by the US Department of Defense (DoDPRMRP) grant PR023081/DAMD17-03-1-0172 and by the Consortium of the Clemson University Center for Bioelectronics, Biosensors and Biochips. KEG thanks the Clemson C3B for a Visiting Professorship and SHC for a transient graduate studentship.

In addition, SHC acknowledges financial support from the Dasan Global Explorer Program (GIST, South Korea).

#### References

- [1] K.E. Geckeler, E. Rosenberg, Functional Nanomaterials, American Scientific Publisher, Valencia, 2006.
- [2] C.S.S.R. Kumar, in: C.S.S.R. Kumar (Ed.), Nanotechnologies for the Life Sciences, Wiley-VCH, Weinheim, 2006.
- [3] K.E. Geckeler, Advanced Macromolecular and Supramolecular Materials and Processes, Kluwer Academic/Plenum, New York, 2003.
- [4] T.J. Mason, J.P. Lorimer, Applied Sonochemistry: Uses of Power Ultrasound in Chemistry and Processing, Wiley-VCH Verlag GmbH, Weinheim, 2002.
- [5] B. Bek, K. Gen, Process Biochem. 35 (9) (2000) 1037–1043.
- [6] P.B. Stathopoulos, et al., Protein Sci. 13 (11) (2004) 3017–3027.
- [7] M.D. Gouda, et al., J. Biol. Chem. 278 (27) (2003) 24324–24333.
- [8] J. Bao, et al., Biochem. Eng. J. 8 (2) (2001) 91–102.
- [9] J. Liu, S.Y. Chan, P.C. Ho, J. Clin. Pharm. Ther. 24 (1999) 145–150.
- [10] N. Vasileva, T. Godjevargova, Mater. Sci. Eng. C 25 (1) (2005) 17–21.
- [11] G. Dai, J. Li, L. Jiang, Colloid Surf. B: Biointerfaces 24 (3–4) (2002) 171–176.
- [12] J.H. Pazur, K. Kleppe, Biochemistry 3 (4) (1964) 578–583.
- [13] A. Guiseppi-Elie, C. Lei, R.H. Baughman, Nanotechnology 13 (5) (2002) 559–564.
- [14] C. Wong, K. Wong, X. Chen, Appl. Microbiol. Biotechnol. 78 (6) (2008) 927–938.
- [15] J.D. Newman, A.P.F. Turner, Biosens. Bioelectron. 20 (12) (2005) 2435–2453.
- [16] F. Scheller, et al., Anal. Chem. 57 (8) (1985) 1740–1743.
- [17] R.A. Bullen, et al., Biosens. Bioelectron. 21 (11) (2006) 2015–2045.
- [18] C.F.B. Witteveen, M. Veenhuis, J. Visser, Appl. Environ. Microbiol. 58 (4) (1992) 1190–1194.
- [19] R. Uppoor, P.J. Niebergall, E.R. James, Pharm. Dev. Technol. 6 (1) (2001) 31–38.
- [20] S. Massa, et al., World J. Microbiol. Biotechnol. 17 (3) (2001) 287–291.
- [21] G.J. Pickering, D.A. Heatherbell, M.F. Barnes, Food Res. Int. 31 (10) (1998) 685–692.
- [22] A. Uzman, Biochem. Mol. Biol. Educ. 29 (2001) 126–128.
- [23] H.U. Bergmeyer, K. Gawehn, M. Grassl, Methods of Enzymatic Analysis, Academic Press Inc., New York, 1974, pp. 457–458.
- [24] J.T. Yang, et al., Methods in Enzymology, Academic Press, 1986, pp. 208–269.
- [25] J. Raso, et al., Ultrason. Sonochem. 5 (4) (1999) 157–162.
- [26] G. Zoldak, et al., J. Biol. Chem. 279 (46) (2004) 47601–47609.
- [27] N.D. Denslow, P.T. Wingfield, K. Rose, Curr. Protoc. Protein Sci. Vol. (1995), 7.1.1–7.1.13.
- [28] R.M. de la Casa, et al., Biotechnol. Tech. 12 (11) (1998) 823–827.
- [29] R.C. Bateman Jr., J.A. Evans, J. Chem. Educ. 72 (12) (1995) A240–A241.
- [30] C. Simpson, et al., Protein Exp. Purif. 51 (2) (2007) 260–266.
- [31] G. Dai, J. Li, L. Jiang, Colloid Surf. B: Biointerfaces 13 (2) (1999) 105–111.